Elsevier Editorial System(tm) for Journal of Luminescence
Manuscript Draft

Manuscript Number:

Title: Linear optical, luminescence and electronic properties of the La2Be2O5 laser crystals doped with Ce3+ or Eu3+

Article Type: Research Paper

Section/Category: LED/OLED phosphors + phosphors + scintillator/thermoluminescence/dosimetry/afterglow

Keywords: Lanthanum beryllate; trivalent cerium and europium; optical absorption spectra; photoluminescence spectra; energy level location

Corresponding Author: Prof. Igor N Ogorodnikov, PhD, Dr.Sc.Hab.

Corresponding Author's Institution: Ural Federal University

First Author: Igor N Ogorodnikov, PhD, Dr.Sc.Hab.

Order of Authors: Igor N Ogorodnikov, PhD, Dr.Sc.Hab.; Vladimir A Pustovarov, PhD, Dr.Sc.Hab.

Abstract: The linear optical, luminescence and electronic properties of La2Be2O5 (BLO) single crystals doped with Ce or Eu, were determined using optical absorption and luminescence spectroscopy techniques. On the basis of the obtained data, the locations of 4f and 5d energy levels for trivalent Ce3+ and Eu3+ impurity ions, and the energy thresholds for 4f->5d and charge transfer transitions were determined for BLO single crystal. The expected positions of the ground states of the 4f[n] and 4f[n-1]5d levels of trivalent lanthanide ions as well as the 4f[n+1] and 4f[n]5d levels of divalent ions were calculated for all the lanthanide ions in BLO host crystal.

Linear optical, luminescence and electronic properties of the $La_2Be_2O_5$ laser crystals doped with Ce^{3+} or Eu^{3+}

I.N. Ogorodnikov[a,*], V.A. Pustovarov[a]

[a] *Ural Federal University, 19, Mira Street, 620002 Ekaterinburg, Russia*

Abstract

The linear optical, luminescence and electronic properties of $La_2Be_2O_5$ (BLO) single crystals doped with Ce or Eu, were determined using optical absorption and luminescence spectroscopy techniques. On the basis of the obtained data, the locations of 4f and 5d energy levels for trivalent Ce^{3+} and Eu^{3+} impurity ions, and the energy thresholds for $4f \rightarrow 5d$ and charge transfer transitions were determined for BLO single crystal. The expected positions of the ground states of the $4f^n$ and $4f^{n-1}5d$ levels of trivalent lanthanide ions as well as the $4f^{n+1}$ and $4f^n5d$ levels of divalent ions were calculated for all the lanthanide ions in BLO host crystal.

Keywords:
Lanthanum beryllate, trivalent cerium and europium, optical absorption spectra, photoluminescence spectra, energy level location

*Corresponding author. Tel.: +7 (343) 3754711; fax: +7 (343) 3743884.
Email address: i.n.ogorodnikov@gmail.com (I.N. Ogorodnikov)

1. Introduction

Considerable interest in lanthanum beryllate $La_2Be_2O_5$ (BLO) arose after revealing the bright effect of stimulated emission in BLO:Nd [1–3], and successful using BLO:Ce in solid state dosimetry of ionizing radiation as a fast inorganic scintillator [4]. Currently, the use of scintillation detectors operating in the spectrometric mode with high energy resolution is crucial for many practical applications. In many cases, these detectors are based on the use of $LaBr_3$:Ce crystals [5–7] or SrI_2:Eu crystals [8–10]. From [4] it follows that BLO crystal doped with Ce^{3+} ions, is also potential candidate for such applications. High chemical and radiation resistance, high melting point (1361°C), optical transparency in a wide spectral range (0.24–5.8 μm) [11], well reproducible technique for growing large single crystals of high optical quality [12], allow one to consider BLO as a promising optical material. However, experimental data on the spectroscopy of BLO single crystals doped with lanthanide ions, are quite limited. Spectroscopic studies BLO:Nd^{3+} and BLO:Pr^{3+} were performed for the visible spectral range [1, 3, 11]. In the host absorption region ($E > 5.8$ eV), the optical properties, and luminescence excitation spectra for the pristine and Ce^{3+} doped BLO crystals were briefly studied in [13–15]. The pulse cathodoluminescence spectra and kinetics for doped BLO crystals were studied in [16, 17]. Optical properties of BLO were discussed in [3, 18]. Data on the study of the BLO electronic structure are relatively scarce. We are aware of only one research work [19], which dealt with the experimental (X-ray photoelectron spectroscopy) and theoretical (LCAO-MO) study of the electronic structure of BLO single crystals. Experimental study of low-temperature ($T = 10$ K) reflection spectra, calculations of the dispersions of the optical constants, refinement of the band gap ($E_g = 6.8$ eV at 10 K) were performed for BLO single crystals in [20].

The aim of this research work is to obtain spectroscopic data on the electronic structure properties of the cerium or europium impurity ions in the BLO host lattice, in particular data on the location of 4f and 5d levels of the impurity ions regarding the energy levels of the host lattice. The paper presents the spectroscopic study (optical absorption spectra; PL emission and PL excitation spectra) of the cerium and europium impurity ions in the BLO host lattice upon excitation in the energy range of the lowest-energy 4f–4f and 4f–5d transitions. On the basis of the experimental data, we determined the locations of 4f and 5d levels for the trivalent cerium and europium impurity ions regarding the energy levels of the BLO host lattice. In the framework of semi-empirical model [21–23] we calculated locations of 4f and 5d levels for all divalent and trivalent lanthanides in

the BLO host lattice.

2. Experimental details

All the examined BLO single crystals of optical quality were grown by V. N. Matrosov using Czochralski method at the Institute of Geology and Geophysics of SB RAS (Novosibirsk, Russia) [12]. The grown BLO crystals were first inspected by X-ray techniques (see details in [12]). The BLO single crystals possess monoclinic crystallographic system, space group symmetry is $C2\bar{c}$ (Z= 4). Lattice parameters are as follows: a= (7.5356 ± 0.0006) Å, b= (7.3476 ± 0.0017) Å, c= (7.4387 ± 0.0006) Å; β= 91.33°; V_μ= 102.94 Å^3; specific weight ρ= 6.061 g/cm^3; molar mass M= 375.82. The BLO crystal structure is formed by corner-shared distorted BeO_4 tetrahedra, La^{3+} ions are asymmetrically embedded into these tetrahedra (point group is C_1). Each La^{3+} ion is coordinated by ten oxygen ions (the distance between atoms varies from 2.415 to 2.999 Å). The crystallographic data are consistent with the earlier data [24].

We used single crystals of lanthanum beryllate: undoped (BLO), doped with trivalent impurity ions (0.5 at %) of cerium (BLO:Ce^{3+}) and europium (BLO:Eu^{3+}). In certain cases, spectroscopic measurements were performed for BLO:Ce (0.05 at %) crystals. Samples for spectroscopic measurements were prepared in the form of polished discs (⊘ 10–15 mm, the sample thickness of l= 1.0 mm) of optical quality.

All measurements were performed at the laboratory of Solid State Physics of Ural Federal University (Yekaterinburg, Russia).

The DFS-13 high-resolution diffraction spectrograph with inverse linear dispersion of 2 Å/mm was used to record the photoluminescence (PL) spectra of the narrow spectral lines from intraconfigurational 4f–4f transitions in BLO:Eu^{3+}. Ultrahigh-pressure xenon lamp DKSSh-1000 was used as the excitation source. In other cases, the PL emission spectra and PL excitation spectra in the energy range of 1.2–6 eV, as well as the temperature dependence of the PL intensity were recorded using a MDR-23 type monochromator with inverse linear dispersion of 13 Å/mm and a R638-10 (Hamamatsu) type photoelectron multiplier tube. In this case, a 400 W deuterium discharge lamp (DDS-400) and the primary double-prism monochromator (DMR-4) were used for luminescence excitation. PL excitation (PLE) spectra are normalized to an equal number of photons incident on the sample, using a sodium salicylate — luminophore with a unit quantum yield in the energy range studied.

Optical absorption spectra were recorded at room temperature by the means of a Heλios Alpha 9423UVA1002E spectrophotometer (λ = 190–1000 nm) equipped

with the Vision 32 software. The narrow spectral lines in the absorption spectra of 4f–4f transitions were recorded at $T = 80$ K by means of a streamlined BECKMAN UV-5270 spectrophotometer. The optical absorption coefficient α was calculated using the formula $\alpha = -\ln(\tau)/l$, where τ is the optical transmittance.

3. Experimental results

3.1. Optical absorption spectra

Pristine undoped crystals. Figure 1 shows the optical absorption spectra recorded for BLO single crystals at $T = 290$ K. Analyzing these spectra, the cutoff energy (E_c), where the value of the absorption coefficient $\alpha = 1\,\text{cm}^{-1}$, was used as the characteristic energy threshold for optical transitions. From the calculated data for the Urbach tail of the fundamental absorption of BLO crystals, obtained in our previous research work [20], it follows that the low-energy edge of the host absorption of pristine undoped BLO crystals at room temperature is located at $E_c = 5.25$ eV, Fig. 1 (curve *5*). The location of the low-energy edge of the host absorption of the optically perfect BLO single crystals at 290 K corresponds to $E_{ca} = 4.9$ eV (Fig. 1 (curve *1*). This difference between the experimental (E_{ca}) and calculated (E_c) values is due to the contribution of unidentified defects with the optical absorption band located at $E > 4.9$ eV near the of low-energy edge of the host absorption.

Cerium doped crystals. Cerium impurity ions in BLO single crystals isomorphically substitute La^{3+} host ions at the C_1-symmetry sites and can be found in two different charge states: Ce^{3+} and Ce^{4+} [13, 14]. The concentration ratio for Ce^3+ and Ce^{4+} ions in the just-grown BLO:Ce crystals depends on various factors including the heat treatment parameters (temperature, annealing time, atmosphere and so on). To obtain a preferential charge state of the cerium impurity ions, we used the pristine BLO:Ce crystals with lowest possible cerium content (0.05 at%), heat treatment was carried out for 15 minutes. Crystals with a dominant Ce^{3+} charge state (BLO:Ce^{3+} crystals) were produced by a reducing heat treatment at $T = 900\,^\circ$C in vacuum. For preferential Ce^{4+} charge state (BLO:Ce^{4+} crystals), the pristine BLO:Ce crystals were subjected to oxidative heat treatment at $T = 600\,^\circ$C in air atmosphere. An excess positive charge of the Ce^{4+} ions in this case is compensated by a corresponding amount of negative oxygen ions.

Figure 1 (curve *2*) shows the optical absorption spectrum recorded for BLO:Ce^{3+} crystal at 290 K. Because of the low symmetry (C_1), all five 5*d*-levels are non-degenerate and should be observed in the absorption spectrum. The experimental

absorption spectrum (Fig. 1, curve *2*) shows three partially overlapped broad absorption bands at 3.5–3.7, 3.8–4.1 and 4.3–4.8 eV. It is worth noting that these bands are due to 4f–5d optical transitions in Ce^{3+} impurity ions. The threshold energy for these transitions is E_{fd}= 3.45 eV. Further refinement of the 4f–5d absorption bands for Ce^{3+} ions in BLO crystals will be done with the following study of PLE spectra (see section 3.2). Optical absorption in the energy range of $E > 4.9$ eV is due to the contribution from unidentified defects, the host absorption of the crystal starts at $E > 5.25$ eV.

Figure 1 (curve *3*) shows the optical absorption spectrum recorded for BLO:Ce^{4+} crystal at 290 K. The broad structureless band with a maximum of about 4 eV is responsible for the absorption of Ce^{4+} ions. The optical absorption is caused by photoinduced optical transitions with charge transfer from the $2p$-orbitals of oxygen to the unoccupied $4f$-orbital of cerium ion in compliance with the scheme [25]

$$Ce^{4+} + O^{2-} \rightarrow Ce^{3+} + O^{-}. \quad (1)$$

The energy E_{CT1}= 2.45 eV can be taken as the threshold energy for the charge-transfer transitions, according to the scheme (1). From Fig. 1 (curve *3*), it is seen that the charge transfer optical transitions occur at energy $E > E_{CT1}$. Such optical transitions involving Ce^{4+} ion, have been previously observed in many crystals, see e.g. [26].

Europium doped crystals. Europium impurity ions isomorphically substitute La^{3+} host ions at the C_1-symmetry sites in BLO single crystals. The broad structureless optical absorption band dominates the absorption spectrum and extends from E_{CT2}= 3.41 eV to the low energy edge of the host absorption of the BLO crystal, Fig. 1 (curve *4*). It is due to charge transfer optical transitions from the surrounding oxygen ions to Eu^{3+} impurity ion

$$O^{2-} + Eu^{3+} \rightarrow O^{-} + Eu^{2+}. \quad (2)$$

The characteristic line-like spectrum of trivalent Eu^{3+} ions is recorded at energies $E < E_{CT2}$, and the absorption coefficient in this energy range is several dozen times lower than that in the charge transfer absorption band. In this regard, the optical absorption in the energy range of $E < E_{CT2}$ was studied using high-aperture spectrophotometer with a spectral resolution of 0.8 nm. Figure 2 presents optical absorption spectra registered at T= 80 K for lanthanum beryllate single crystal doped with europium (0.5 at%). For convenience, the analysis of line-like spectra (Fig. 2) was done using the wavelength coordinates at the abscissa axis.

This spectrum confidently identify the optical transitions $^7F_0 \rightarrow {}^5D_j$ (j= 1–4), $^7F_0 \rightarrow {}^5G_{2,3}$, $^5L_{6,7}$, corresponding to the electronic transitions in the Eu^{3+} ion. In the future, such crystals will be denoted as BLO:Eu^{3+}. It is worth noting that in this study we did not intend to produce and investigate divalent europium impurity ions in BLO single crystals.

3.2. PL emission and excitation spectra

Cerium doped crystals. Photostimulation in the 4f–5d absorption band of BLO:Ce^{3+} crystals leads to the fast intense luminescence, which is concentrated in the complex broad band of PL emission at 2.2–2.8 eV with the observed maximum of about 2.52 eV. PL quantum yield upon excitation is η= 0.4 relative to sodium salicylate. PL emission band parameters (intensity and spectral shape) depend on the temperature and excitation energy.

Figure 3 shows PL emission spectra recorded for theBLO:Ce^{3+} crystal at temperatures T = 80 and 290 K and excitation energies E_{ex}, corresponding to the three 4f–5d absorption bands shown in Fig. 1 (curve *2*). Each PL emission band (Fig. 3) consists of two elementary Gaussian-shape bands, the best fit parameters are presented in Tab. 1. First dominant elementary band is located at 2.51–2.52 eV. The second band at 2.81–2.82 eV has lower amplitude. The ratio of their intensities is 3.2–4.9 at 80 K and 4.6–6.9 at 290 K. The energy gap between the positions of the maxima of these PL emission bands is ΔE_{so}= 0.28–0.30 eV at 80 K and 0.31 eV at 290 K.

It is known [27] that the luminescence spectra of Ce^{3+} ions are caused by radiative transitions $5d \rightarrow 4f$, which usually appear as a doublet of the broad, partially overlapped emission bands. These PL emission bands are due to radiative transitions from the lowest relaxed $5d$-excited state to the ground $4f$ state, split by the spin-orbit interaction onto the two levels of $^2F_{5/2}$ and $^2F_{7/2}$. This splitting for free Ce^{3+} ion is around 2200 cm^{-1} (0.27 eV) [27]. In condensed matter its value depends on many factors and varies from crystal to crystal, but its mean value is again about 0.27 eV [28]. This is entirely consistent with the resulting values in our measurements 0.28–0.31 eV (Tab. 1).

PL excitation spectra (Fig. 3, curves *5* and *6*) comprise a complex broad band extending from 3.2 to 5.5 eV. One can recognize two energy intervals in the PLE spectra: (I) 3.2–4.2 eV corresponds to the most efficient excitation of this PL, (II) 4.2–5.2 eV, PL excitation efficiency in this field decreases approximately by 3–5 times. Decomposition of the PLE spectrum (Tab. 2) has revealed five elementary partially-overlapped Gaussian-shape bands, combined into two groups. Energy interval I contains a group of three bands G1–G3, which from a practical point

of view should be considered as equidistant bands (E_{ex}= 3.51, 3.74, 4.05 eV) of equal full width (FWHM= 0.26–0.32 eV). Here, E_{ex} is the energy position of the Gaussian-shape band maximum. In energy interval II, there are two low-intensity bands G4 and G5 at 4.51 and 5.08 eV (FWHM= 0.44 and 0.47 eV).

Analysis of the spectroscopic data (Fig. 3) indicates that the intense luminescence of BLO:Ce^{3+} crystal in the visible spectral region is due to radiative transitions in Ce^{3+} impurity ion. Indeed, the free Ce^{3+} ion has $4f^1$ configuration of the ground state and lowest excited $5d^1$ state at 5.9 eV. For Ce^{3+} ion in the crystal host, the lowest-energy $4f^1 \rightarrow 5d^1$ allowed electro-dipole transitions can be observed in the energy range from 2.5 to 4.95 eV, depending on the specific properties of the host and the symmetry of the impurity ion site [29, 30]. Interconfigurational $5d \rightarrow 4f$ transitions in Ce^{3+} ion are dominant radiative transitions in crystals containing Ce^{3+} ions. The final stage of the radiative process obeys the scheme

$$\left(Ce^{3+}\right)^{*} \rightarrow Ce^{3+} + h\nu. \tag{3}$$

For intracenter photoluminescence excitation of Ce^{3+} ions, this scheme is only one possible. The full width of $5d$ band is typically about 15000 cm^{-1} (1.86 eV) [27]. It is worth noting that all five PLE bands (Fig. 3) are well within the energy range from E_{fd}= 3.45 eV to (E_{fd} + 1.86)= 5.31 eV.

Figure 4 (curves *1* and *2*) shows the temperature dependences of PL intensity recorded for BLO:Ce^{3+} single crystal monitoring emission at 2.53 eV (d–f PL emission band of Ce^{3+} in BLO) upon photoexcitation at 3.6 and 5.4 eV. Upon excitation to the lowest $5d$ states, the temperature dependence of the PL yield (Fig. 4, curve *1*) obeys the Mott law with an activation energy of E_a= 0.38 eV. This corresponds to the activation energy for the intracenter quenching of the PL emission. However, during the excitation of the upper $5d$ states, the luminescence yield drops on cooling the crystal (it's maximum is located in the temperature range of 300–350 K, Fig. 4 (curve *2*). This can be explained by photoionization of Ce^{3+} ions due to the partial overlapping the upper $5d$ states with the conduction band. Capturing of such photoelectrons by an external trap can be a possible reason for the decrease in the luminescence yield with decreasing temperature.

It is worth noting that the PL decay kinetics for BLO single crystals doped with cerium impurity ions, has been investigated previously in our work [15]. From [15] it follows that the PL decay kinetics recorded for BLO:Ce crystal at T= 300 K and E_{ex}= 4.7 eV monitoring emissions in the energy range of the d-f emission band of Ce^{3+}, is single exponential with lifetime τ= 29 ns, and exhibits no inertial decay stages. In the present study, we are focusing on other issues.

Europium doped crystals. Figure 5 shows PL emission spectrum of BLO:Eu^{3+} single crystal recorded at $T = 80$ K with a spectral resolution of 0.8 nm upon photoexcitation at 3.90 eV. Analysis of spectral and luminescent properties of BLO:Eu^{3+} allows us to draw some additional conclusions on the crystal structure of this compound. Indeed, the presence of no splits in the crystal field levels for the $^5D_0$ and $^7F_0$ levels, is often determine the use of Eu^{3+} ion as a luminescent probe for the study of crystallographic structure. Registration in the PL emission spectrum of only one line for the radiative $^5D_0 \rightarrow {}^7F_0$ transition indicates that all Eu^{3+} ions in BLO are in equivalent positions. Several factors speak in favor of the low symmetry of the luminescence center: namely, the shape of the PL emission spectrum; magnetic dipole transition $^5D_0 \rightarrow {}^7F_1$ dominates the spectrum; the number of spectral lines is close to the limit. A characteristic feature of the Eu^{3+} luminescence in BLO is a non-radiative energy relaxation from highly excited levels to the lowest excited $^5D_0$ state. Radiative transitions are only observed from this level. It is worth noting that the relatively high emission intensity exhibit radiative transitions onto the upper ($^7F_3$ and $^7F_4$) levels of the ground term.

Figure 6 shows PLE spectrum recorded for BLO:Eu^{3+} single crystal at 80 K monitoring emission in the energy interval of 1.9–2.0 eV. Along with narrow lines corresponding to excitation of $^5D_{1-3}$, $^5L_6$ levels, the PLE spectrum at $E > E_{CT2}$ shows a broad PLE band corresponding to electronic charge-transfer transitions O–Eu (CT-band). Cutoff energy of CT-band recorded for the low-energy side, is consistent with the value of the low energy threshold for CT-transitions (E_{CT2}), determined from the optical absorption spectra (Fig. 1). The energy position of the CT-band maximum in PLE spectra is about 4.1 eV, Fig. 3. It is worth noting that the CT-band O–Eu is not only the dominant PLE band for excitation of Eu^{3+} emission in BLO, but it has also an elevated thermal stability in the investigated temperature range from 80 to 290 K. Short energy interval of PLE spectrum in the energy region of 3.0–3.6 eV, which is observed only at $T = 80$ K, is due to excitation of Eu^{3+} ions through 4f–4f transitions as indicated in Fig. 6.

Figure 4 (curve *3*) shows the temperature dependence of the PL intensity recorded for BLO:Eu^{3+} single crystal monitoring emission in the energy region of 1.9–2.0 eV upon photoexcitation at 3.1 eV. From this dependence it follows that the PL intensity has a maximum at about 160 K. At $T = 80$ K, the PL intensity decreases by 1.7 times. On heating to $T = 480$ K, the PL intensity decreases by the factor of about 14 and the curve becomes saturated. Falling plot of the temperature curve at $T > 160$ K can be approximated by the Mott law with an activation energy of $E_a = 0.17$ eV. However, a more detailed study of the temperature dependence for the 4f–4f transitions in Eu^{3+} ions in BLO is a separate independent problem that

are not directly related to the purpose of the present study.

4. Discussion

4.1. Location of lanthanide energy levels

Electronic energy structure of BLO. Intrinsic lowest-energy electronic excitations in luminescent materials are usually due to electronic transitions from the states of valence band (VB) top onto the states of conduction band (CB) bottom. The probability of such transitions is determined by the origin of the initial and final electronic states. Bandgap E_g= 6.8 eV has been determined for BLO single crystals from the low-temperature (T= 10 K) reflection spectra [20]. According to the calculated data [19], the electronic structure of BLO single crystal in the vicinity of the VB top is due to hybridized states including O 2p, La 5d, 6s and Be 2p atomic orbitals. We are not aware of calculated data on electronic structure of CB for BLO single crystals, therefore we discuss the experimental data. On the bases of the low-temperature reflection spectra recorded at T= 10 K) for BLO single crystals Pustovarov et al. [20] have found that the lowest-energy electronic transitions in BLO are caused by electron transfer from the VB top states onto the La 3d states forming the CB bottom and La 6s states located at 3.5 eV above the CB bottom. It is worth noting that in many borate compound, the CB bottom consists of antibonding hybridized O 2p- and B 2p-orbitals, as well as d-orbitals of metal cations [31]. The result is a mixed $p\,d$ character of the lowest-energy electronic excitations, manifesting the absence of pronounced excitonic states in the low energy tail of the host absorption. Owing to this, the CB bottom in the binary oxide Sc_2O_3 is formed by 3d-orbitals of scandium, whereas the VB top comprises of 2p orbitals of oxygen, so this crystal, in contrast to the isostructural compound Y_2O_3, does not exhibit neither excitonic absorption nor excitonic luminescence [32]. The low-energy tail of the host absorption in barium metaborate β–BaB_2O_4 also does not exhibit any manifestations of exciton states [33]. The lack of manifestations of the excitonic states in the reflection and PLE spectra of BLO in the energy range of 6.2–6.8 eV, which was found earlier in [15, 20], can serve as an indirect indication of the significant contribution d states of metal cations into the electronic structure of the states near the CB bottom of BLO.

Experimental data on the luminescence spectroscopy obtained in the present work we will use to further refinement of the electronic structure and positions of the levels of lanthanides in the BLO single crystals. Figure 7 shows the final result of this refinement. We will consider in more detail the key stages of the construction of this diagram.

$4f^n \rightarrow 4f^{n-1}5d$-transitions. Electronic structure of free lanthanide ions (Ln) is well known, studied in detail and its description can be found in many publications and monographs, see. e.g. [34]. Internal $4f$ orbitals of the lanthanides are well shielded from external influences. Electronic energy structure of $4f$ states is described by the extended Dieke diagram [35]. The introduction of an ion into the host crystal, the position of $4f$-levels changes very little, less than $100\,\mathrm{cm}^{-1}$ (about 0.01 eV). In this regard, in most cases, characterization of $4f$ states of the ion only requires determining the position of its ground $4f^n$-state in the crystal host (here n is number of electrons for $4f$ shell). For divalent Ln^{2+} ion this state can be located above the CB bottom or in band gap above the Fermi level. For trivalent Ln^{3+} ion the ground $4f^n$-state can be located within the band gap below the Fermi level or below the VB top [23].

Location of $5d$ excited levels of trivalent lanthanides in inorganic hosts with respect to the location of the ground $4f^n$ state is strongly influenced by the crystalline environment and may vary from crystal to crystal to tens of thousands of inverse centimeters (a several few eV). The threshold energy for $4f^n \rightarrow 4f^{n-1}5d$ transition (ΔE_{fd}) for the Ln^{3+} ion in the crystal host is determined by the formula [36]

$$\Delta E_{\mathrm{fd}} = \Delta E^*_{\mathrm{fd}} - D, \tag{4}$$

where ΔE^*_{fd} is the threshold energy for $4f^n \rightarrow 4f^{n-1}5d$ transition in free Ln^{3+} ion, Tab. 2; D is a red spectroscopic shift. From our experimental data (Fig. 1) it follows that the threshold energy for $4f^1 \rightarrow 5d$ transition for Ce^{3+} ion in BLO single crystal is $\Delta E_{\mathrm{fd}}\,(Ce^{3+}) = E_{\mathrm{fd}} = 3.45$ eV ($27826\,\mathrm{cm}^{-1}$). Spectroscopic shift value D is the characteristic of the host, it is determined only by the properties of the host and is the same for all Ln^{3+} ions in this host. Substituting the value D in the formula (4), we calculated the threshold energy for $4f^n \rightarrow 4f^{n-1}5d$ transitions of Ln^{3+} ions in the BLO host, Fig. 7.

Charge-transfer transitions. Electron transfer from the VB top (ligand, L) to the unfilled f or d orbital of the metal (M) cation leads to the 'ligand to metal' charge-transfer transition (LMCT). Such transitions are partially resolved and appear as a very broad band of optical absorption in the ultraviolet energy range. Parameters of the charge transfer band dependent on optical electronegativity of ligands, electron affinities of the cations, and a distance between these cation and ligand. The threshold energy for the charge-transfer transition in optical absorption can be calculated by the formula [37]

$$E_{\mathrm{CT}} = (\chi(\mathrm{O}) - \chi(\mathrm{Ln})) \times 3.72\,\mathrm{eV}, \tag{5}$$

where χ(O), χ(Ln) are the optical electronegativities of the atoms of oxygen and Ln cation. According to [38], χ(O)= 3.2 and χ(Eu)= 1.75. In this case, the assessment of location of CT-band O–Eu is approximately 5.3 eV. This relation is fairly correct for many of the rare earth elements, such as Eu^{3+} ions in some compounds. Two important facts have been established empirically for the host crystals doped with europium. Firstly, E_{CT} in the host crystals corresponds to the energy position of the $4f^7$ ground level of divalent Eu^{2+} ion with respect to the VB top; Secondly, the $4f^7$ ground level of Eu^{2+} ion in the host crystals, is located lower in energy than $4f^5 5d^1$ level of trivalent Eu^{3+} ion [23, 39, 40]. In oxide compounds, charge-transfer transition $O^{2-} \rightarrow Eu^{3+}$ is due to electron transfer from the O $2p$ states of VB top onto the $4f^7$ ground state of Eu^{2+} ion [22, 41, 42].

Many compounds show a significant deviation of the experimental value (E_{CT}) in comparison with the values calculated by the formula (5). It is worth noting that the exact position of the CT-band depends not only on the parameters of the ions, but also on the properties of the host crystal. Thus, the energy position of the CT-band is red-shifted with increasing ion radius of occupied positions and distances between the impurity and oxygen ions [38]. More rigorous calculation of the energy position of CT-band for the Eu ion in eightfold coordination predicted values from 4.5 to 5.6 eV for different host crystals [43]. Experimental data on the energy positions of CT-band O–Eu for some host crystals: 4.6 ($GdBaB_9O_{16}$ [44]), 4.63 ($Li_6Gd(BO_3)_3$ [45–47]), 4.98 eV ($Li_6Y(BO_3)_3$ [45]). As a result, the charge transfer position is sensitive to the ion environment and it can vary from host to host over a broad range. Dorenbos [21, 22] showed that possible CT energy is in the range from 3.3 to 6.5 eV. These data are consistent with our experimental data. The broad optical absorption band for the charge-transfer transitions $O^{2-} \rightarrow Eu^{3+}$ in BLO crystal is observed in the energy region of 3.4–5.4 eV. At 290 K, the low-energy cutoff is located at E_{CT2}= 3.41 eV, Fig. 1, and the CT-band maximum is located at 4.1 eV, Fig. 6.

Locations of the $4f^n$ and $4f^{n-1}5d$ energy levels in BLO single crystal. Analysis of the experimental data on BLO:Ce and BLO:Eu (Fig. 1 – Fig. 6) allows us to make justified conclusions about the locations of $4f^n$ and $4f^{n-1}5d$ ground levels in BLO crystal. Let us briefly discuss the results of this analysis.

The $4f^1$ ground level of Ce^{3+} ion in wide-gap crystals is usually located above the VB top. In addition to Ce^{3+} ions, BLO:Ce crystal also contains Ce^{4+} ions associated with the charge-balancing lattice defects. From general considerations, it is obvious that the energy of the $4f^1$ ground state of Ce^{3+} ion in the complex

defect will be slightly higher than the energy for the same ion in a regular position in the defect-free area of a crystal. However, the energy threshold for charge-transfer transitions was reliably determined in our experiment: $E_{CT1} = 2.45$ eV, Fig. 1. In this connection, the charge-transfer transitions between the VB top and the $4f$ vacant state of Ce^{4+} ion, we used to determine the position of the $4f^1$ ground state of Ce^{3+} ion in BLO crystal.

Semiempirical model [22, 23] describes the relationship between the energy values of $4f^n$ ground levels for different lanthanides in the same host. If we can determine the energy value of the $4f^n$ ground level for one rare-earth ion, we can calculate the energy of the $4f^n$ ground levels for other lanthanide ions in the same host. According to [22], the systematic energy shift between the $4f^n$ ground levels of Ce^{3+} and Eu^{3+} ions is $\Delta E^{Eu,\,Ce} = 35900\,cm^{-1}$ (4.45 eV). In this case, the $4f^6$ ground level of Eu^{3+} ion in BLO single crystal should be located at 2.0 eV below the VB top ($2.45 - 4.45 \approx -2.0$ eV), Fig. 7.

The $4f^1$ ground state of Ce^{3+} ion is split by spin-orbit interaction into two levels $^2F_{5/2}$ and $^2F_{7/2}$, Fig. 7. The results obtained in our measurements ($\Delta E_{SO} = 0.28$–0.31 eV, Tab. 1) are sufficiently close to the expected value of 0.27 eV.

To determine the energy location of $5d$ level of Ce^{3+} ion in BLO crystal host, we used the experimental value of the threshold energy for $4f^1 \rightarrow 5d$ transition in Ce^{3+} ion, constituting $E_{fd} = 3.45$ eV, Fig. 1. Location of $5d$ level in Ce^{3+} ion must be at $(2.45 + 3.45\,eV) = 5.90$ eV above the VB top in BLO. Model [22, 23] describes the relationship between the energy values for $4f^{n-1}5d$ levels for different lanthanides in the same host. If we know the energy of $4f^{n-1}5d$ level for one rare-earth ion, we can calculate the energy of the $4f^{n-1}5d$ levels for other lanthanides in the same host. All calculated values (Fig. 8, curve *2*) were located close to the energy of 5.90 eV, established above for $5d$ level of Ce^{3+} ion in BLO. This is not surprising, since the energy location of the $4f^{n-1}5d$ level of lanthanides in the same host is determined mainly by the crystal field and practically does not depend on the kind of $4f$ ion with the same charge state [22, 23, 39, 40].

Within the framework of semiempirical model [22, 36], the definition of the energy locations of the ground levels for Ce^{3+} and Eu^{3+} ions allowed us to calculate the expected energy locations of the ground levels for all lanthanides in BLO crystal. Figure 8 shows the results of calculation. The energy location of the $4f^7$ ground level of Eu^{2+} in BLO:Eu crystal is $E_{CT2} = 3.41$ eV, Fig. 1). On the basis of these data, we have calculated the energy locations of the $4f^n$ and $4f^{n-1}5d$ states in divalent lanthanides for BLO single crystal, Fig. 8 (curves *3* and *4*).

5. Conclusions

Thus, we performed a spectroscopic study of single crystals of lanthanum beryllate doped with cerium or europium impurity ions, upon excitation in the lowest-energy 4f–4f and 4f–5d optical transitions (E_{ex} = 3.0–6.5 eV, T = 80 and 290 K). The most important conclusions are as follows.

1. Along with the line-like spectra of the optical absorption induced by 4f–4f transitions in trivalent Eu^{3+} ions, lanthanum beryllate single crystals show intense broad absorption bands, which are caused by charge-transfer transitions from the ligands to the metal impurity ions. Based on the analysis of optical absorption spectra of BLO single crystals doped with impurity ions of Ce^{3+}, Ce^{4+} or Eu^{3+}, we have defined threshold energies for host absorption (E_{ca} = 4.9 eV), $4f$–$5d$ transition in Ce^{3+} ions (E_{fd} = 3.45 eV), charge-transfer transitions O – Ce^{4+} (E_{CT1} = 2.45 eV) and O – Eu^{3+} (E_{CT2} = 3.41 eV), as well as the spectroscopic red-shift for trivalent Ln^{3+} ions (D = 2.67 eV).

2. Intense (quantum yield relative to sodium salicylate $\eta \approx$ 0.4), fast (τ = 29 ns) luminescence in BLO:Ce single crystals is due to radiative 5d–4f transitions from the lowest excited $5d$ state of the Ce^{3+} ion. Luminescence spectra comprise two partially overlapped PL emission bands at 2.52 and 2.82 eV. The PLE spectrum consists of five bands, corresponding to transitions from the $4f^1$ ground state to the excited $5d$ levels in Ce^{3+} ion.

3. Low-intensity luminescence in BLO:Eu crystals is characterized by a line-like spectrum and a slow PL decay kinetics. This emission is caused by the 4f–4f radiative transitions from the lowest excited state ($^5D_0$) onto the $^7F_{0-4}$ ground state of Eu^{+3} ion. PLE spectrum is concentrated in the energy range of 3–5.5 eV. It comprises a broad band of the dominant charge-transfer transitions O – Eu ($E > E_{CT2}$ = 3.41 eV). This band overlaps partially with the energy area of 3.0–3.4 eV, corresponding to the absorption lines for 4f–4f transitions ($^7F_0 \rightarrow {}^5D_{3,4}$,$^5L_{6,7}$, $^5G_{2,3}$) in ion Eu^{3+}.

Temperature dependence of PL intensity for 5d–4f luminescence of Ce^{3+} ion is characterized by intracenter temperature quenching at $T >$ 300–320 K and obeys the Mott law with an activation energy of E_a = 0.38 eV. Luminescence yield has a maximum in the temperature range of 300–350 K, and upon cooling the crystal it drops. The probable cause is an overlap of the upper $5d$ states and the CB-states in BLO.

4. Based on the experimental data, we have established energy locations for the 4f and 5d levels of trivalent Ce and Eu ions in the BLO single crystals. The $4f^1$ ground state of Ce^{3+} impurity ion is located at 2.45 eV above the VB top, three

lower excited 5d states are located in the crystal band gap at 0.5–1.5 eV below the CB bottom. Two upper excited 5d states are located in the CB of the crystal. The $4f^6$ ground level of Eu^{3+} impurity ion is located at 2.0 eV below the VB top, and the excited $^5D_{0-3}$ and $^5L_6$ states are located above the VB top. Highly-excited 4f states overlap in energy with a broad band of charge-transfer transitions O – Eu. The $4f^5 5d$ state is located at 6 eV above the VB top, so the hypothetical 4f–5d transition energy will overlap with the host absorption region.

The data obtained are in demand for a reasonable interpretation of the experimental data on a study of other impurity ions and recombination processes with their participation in BLO single crystals.

Acknowledgments

The authors are grateful to V. N. Matrosov for providing samples for examination and A. A. Maslakov for assistance in the spectroscopic measurements. This work was partially supported by the Ministry of Education and Science, Russia (the basic part of the government mandate).

References

[1] Y. K. Voronko, G. V. Maksimova, V. V. Osiko, A. A. Sobol, B. P. Starikov, and M. I. Timoshechkin, "Spectroscopic properties of $La_2Be_2O_5$:Nd^{3+} single crystals," Phys. Status Solidi (a) **17**, K41–K43 (1973).

[2] R. C. Morris, C. F. Cline, R. F. Begley, M. Dutoit, P. J. Harget, H. P. Jenssen, T. S. LaFrance, and R. Webb, "Lanthanum beryllate: A new rare-earth ion laser host," Appl. Phys. Lett. **27**, 444–445 (1975).

[3] H. P. Jenssen, R. F. Begley, R. Webb, and R. C. Moris, "Spectroscopic properties and laser performance of Nd^{3+} in lanthanum beryllate," J. Appl. Phys. **47**, 1496–1500 (1976).

[4] J. B. Czirr and M. Berrondo, "Photon detector based upon an activated lanthanide beryllate scintillator," United States Patent 5483062. (09.01.1996). (Mapleton, Orem, UT).

[5] P. Dorenbos, E. V. D. van Loef, A. P. Vink, E. van der Kolk, C. W. E. van Eijk, K. W. Krämer, H. U. Güdel, W. M. Higgins, and K. S. Shah, "Level location and spectroscopy of Ce^{3+}, Pr^{3+}, Er^{3+}, and Eu^{2+} in $LaBr_3$," J. Lumin. **117**, 147–155 (2006).

[6] N. J. Cherepy, S. A. Payne, S. J. Asztalos, G. Hull, J. D. Kuntz, T. Niedermayr, S. Pimputkar, J. J. Roberts, R. D. Sanner, T. M. Tillotson, E. van Loef, C. M. Wilson, K. S. Shah, U. N. Roy, R. Hawrami, A. Burger, L. A. Boatner, W.-S. Choong, and W. W. Moses, "Scintillators with potential to supersede lanthanum bromide," IEEE Trans. Nucl. Sci. **56**, 873–880 (2010).

[7] V. A. Pustovarov, A. N. Razumov, and D. I. Vyprintsev, "Luminescence of $LaBr_3$:Ce,Hf crystals under photon excitation in the ultraviolet, vacuum ultraviolet, and X-ray ranges," Phys. Solid State **56**, 347–352 (2014).

[8] N. J. Cherepy, G. Hull, A. D. Drobshoff, S. A. Payne, E. van Loef, C. M. Wilson, K. S. Shah, U. N. Roy, A. Burger, L. A. Boatner, W.-S. Choong, and W. W. Moses, "Strontium and barium iodide high light yield scintillators," Appl. Phys. Lett. **92**, Art.no.083508 (2008).

[9] V. A. Pustovarov, I. N. Ogorodnikov, A. A. Goloshumova, L. I. Isaenko, and A. P. Yelisseyev, "A luminescence spectroscopy study of scintillation crystals SrI_2 doped with Eu^{2+}," Opt. Mater. **34**, 926–930 (2012).

[10] V. Pankratov, A. I. Popov, L. Shirmane, A. Kotlov, G. A. Bizarri, A. Burger, P. Bhattacharya, E. Tupitsyn, E. Rowe, V. M. Buliga, and R. T. Williams, "Luminescence and ultraviolet excitation spectroscopy of SrI_2 and SrI_2:Eu^{2+}," Radiat. Meas. **56**, 13–17 (2013).

[11] A. A. Kaminskii, T. Ngoc, S. E. Sarkisov, V. N. Matrosov, and M. I. Timoshechkin, "Growth, spectral and laser properties of $La_2Be_2O_5$:Nd^{3+} crystals in the $^4F_{3/2} \rightarrow {}^4I_{11/2}$ and $^4F_{3/2} \rightarrow {}^4I_{13/2}$ transitions," Phys. Status Solidi (a) **59**, 121–139 (1980).

[12] E. G. Tsvetkov, G. M. Rylov, and V. N. Matrosov, "Formation of lanthanum beryllate real structure under different crystallization conditions," Mater. Res. Bull. **41**, 307–318 (2006).

[13] A. V. Kruzhalov, A. A. Maslakov, V. L. Petrov, and B. V. Shulgin, "Temperature features of Ce luminescence yield spectra in lanthanum beryllate," Zh. Prikl. Spektrosk. **45**, 859–861 (1986).

[14] A. V. Kruzhalov, V. A. Pustovarov, A. A. Maslakov, V. L. Petrov, and B. V. Shulgin, "Luminescence excitation and reflection spectra of $La_2Be_2O_5$ crystals in the 5–36 eV region," Opt. Spectrosc. **63**, 268–270 (1987).

[15] V. A. Pustovarov, V. L. Petrov, É. I. Zinin, M. Kirm, G. Zimmerer, and B. V. Shulgin, "Optical and luminescent VUV spectroscopy of $La_2Be_2O_5$ crystals," Phys. Solid State **42**, 253–256 (2000).

[16] D. M. Gualtieri, "Cathodoluminescence of Ce:$La_2Be_2O_5$ single crystals," J. Lumin. **60-61**, 127–130 (1994).

[17] R. Piramidowicz, M. Kowalska, and M. Malinowski, "Energy transfer processes in Pr^{3+}:$Be_2La_2O_5$ crystals," J. Alloys Compd. **300–301**, 430–434 (2000).

[18] M. J. Weber, *Handbook of Optical Materials* (CRC Press, Boca Raton, London, New York, 2003). 500 p.

[19] T. A. Betenekova, A. V. Kruzhalov, N. M. Osipova, V. P. Palvanov, V. L. Petrov, and I. N. Shabanova, "Electron structure and valence band structure of beryllium orthosilicate and lanthanum beryllate," Fiz. tverd. tela **25**, 175–179 (1983).

[20] V. A. Pustovarov, I. N. Ogorodnikov, and E. A. Ospanbekov, "Optical and electronic properties of undoped $La_2Be_2O_5$ single crystals in the far ultraviolet energy range," J. Opt. Soc. Am. B-Opt. Physics (2015). (In Press).

[21] P. Dorenbos, "Systematic behaviour in trivalent lanthanide charge transfer energies," J. Phys.: Condens. Matter **15**, 8417–8434 (2003).

[22] P. Dorenbos, "The Eu^{3+} charge transfer energy and the relation with the band gap of compounds," J. Lumin. **111**, 89–104 (2005).

[23] P. Dorenbos, "Absolute location of lanthanide energy levels and the performance of phosphors," J. Lumin. **122-123**, 315–317 (2007).

[24] L. A. Harris and H. L. Yakel, "The crystal structure of $La_2Be_2O_5$," Acta Crystallogr. Section B **24**, 672–682 (1968).

[25] G. Zhenan, "Spectroscopic properties of doped silica glasses," J. Non-Crystal. Solids **52**, 337–345 (1982).

[26] F. Yang, S. K. Pan, D. Z. Ding, X. F. Chen, S. Lu, W. D. Zhang, and G. H. Ren, "Growth and optical properties of the Ce-doped $Li_6Gd(BO_3)_3$ crystal grown by the modified Bridgman method," J. Alloys Compd. **484**, 837–840 (2009).

[27] G. Blasse and B. C. Grabmaier, *Luminescent materials* (Springer-Verlag Telos, Berlin, 1994). 232 p.

[28] D. Hou, B. Han, W. Chen, H. Liang, Q. Su, P. Dorenbos, Y. Huang, Z. Gao, and Y. Tao, "Luminescence of Ce^{3+} at two different sites in α–$Sr_2P_2O_7$ under vacuum ultraviolet-UV and x-ray excitation," J. Appl. Phys. **108**, 083527(6) (2010).

[29] P. Dorenbos, "Crystal field splitting of lanthanide $4f^{n-1}5d$-levels in inorganic compounds," J. Alloys Compd. **341**, 156–159 (2002).

[30] P. A. Tanner, C. S. K. Mak, N. M. Edelstein, K. M. Murdoch, G. Liu, J. Huang, L. Seijo, and Z. Barandiarán, "Absorption and emission spectra of Ce^{3+} in elpasolite lattices," J. Am. Chem. Soc. **125**, 13225–13233 (2003).

[31] K. C. Mishra, B. G. De Boer, P. C. Schmidt, I. Osterloh, M. Stephan, V. Eyert, and K. H. Johnson, "Electronic structures and nature of host excitation

in borates," Berichte der Bunsen-Gesellschaft-Physical Chemistry Chemical Physics **102**, 1772–1782 (1998).

[32] V. N. Abramov, A. N. Ermoshkin, A. I. Kuznetsov, and V. V. Murk, "Breakdown of excitonic absorption and luminescence induced by a d-type conduction band in Sc_2O_3," Phys. Status Solidi (b) **121**, K59–K63 (1984).

[33] Y.-N. Xu, W. Y. Ching, and R. H. French, "Electronic structure and interatomic bonding of crystalline BBO with comparison to LBO," Phys. Rev. B: Cond. Matter **48**, 17695–17702 (1993).

[34] G. H. Dieke, *Spectra and Energy Levels of Rare Earth Ions in Crystals* (Wiley Interscience, New York, 1968). 401 p.

[35] R. T. Wegh, A. Meijerink, R.-J. Lamminmäki, and J. Hölsä, "Extending Dieke's diagram," J. Lumin. **87-89**, 1002–1004 (2000).

[36] P. Dorenbos, "The 5d level positions of the trivalent lanthanides in inorganic compounds," J. Lumin. **91**, 155–176 (2000).

[37] C. K. Jørgensen, "Electron transfer spectra," Progr. Inorg. Chem **12**, 101–158 (1970).

[38] L. van Pieterson, M. Heeroma, E. de Heer, and A. Meijerink, "Charge transfer luminescence of Yb^{3+}," J. Lumin. **91**, 177–193 (2000).

[39] P. A. Rodny, I. V. Khodyuk, and G. B. Stryganyuk, "Location of the energy levels of the rare-earth ion in BaF_2 and CdF_2," Phys. Solid State **50**, 1639–1643 (2008).

[40] A. Belsky and J. C. Krupa, "Luminescence excitation mechanisms of rare earth doped phosphors in the VUV range," Displays **19**, 185–196 (1999).

[41] X. Wu, H. You, H. Cui, X. Zen, G. Hong, C.-H. Kim, C.-H. Pyun, B.-Y. Yu, and C.-H. Park, "Vacuum ultraviolet optical properties of (Li,Gd)PO_4:RE^{3+} (RE = Eu, Tb)," Mater. Res. Bull. **37**, 1531–1538 (2002).

[42] C. Pédrini, "Electronic processes in rare earth activated wide gap materials," Phys. Status Solidi (a) **202**, 185–194 (2005).

[43] B. Liu, C. Shi, Q. Zhang, and Y. Chen, "Temperature dependence of $GdVO_4$:Eu^{3+} luminescence," J. Alloys Compd. **333**, 215–218 (2002).

[44] Z. Yang, J. H. Lin, M. Z. Su, Y. Tao, and W. Wang, "Photon cascade luminescence of Gd in $GdBaB_9O_{16}$," J. Alloys and Compounds **308**, 94–97 (2000).

[45] M. Leskelä and J. Hölsä, "Luminescence properties of Eu^{3+} doped $Li_6Ln(BO_3)_3$ (Ln=Gd,Y) phosphors," Eur. J. Solid State Inorg. Chem. **28**, 151–154 (1991).

[46] I. N. Ogorodnikov, I. N. Sedunova, A. V. Tolmachev, and R. P. Yavetskiy, "Temperature dependence of the luminescence of $Li_6Gd_xY_{1-x}(BO_3)_3$:Eu crystals," Opt. Spectrosc. **113**, 63–70 (2012).

[47] I. N. Ogorodnikov and V. A. Pustovarov, "Luminescence of $Li_6Gd(BO_3)_3$ crystals upon ultraviolet and inner-shell excitations," J. Lumin. **134**, 113–125 (2013).

Table 1: Best fit parameters of PL emission spectra recorded for BLO:Ce^{3+} single crystals at temperature T upon excitation at energy E_{ex}: energy position of the peak maximum (E_m, eV), FWHM (ΔE, eV), amplitude (A, arb.units).

Experiment		Peak fit parameters		
T, K	E_{ex}, eV	E_m	ΔE	A
80	3.50	2.51	0.39	99.62
		2.81	0.24	20.60
80	3.97	2.52	0.36	74.96
		2.80	0.23	23.42
290	3.50	2.51	0.44	47.83
		2.82	0.33	6.91
290	4.43	2.51	0.42	19.07
		2.82	0.30	4.13

Note. The peak amplitudes were normalized to 100 conventional units at the observed maximum of the most intense PL emission band (Fig. 3, curve 1).

Table 2: Best fit parameters of PL excitation spectra recorded for BLO:Ce^{3+} single crystals at temperature $T = 80$ K monitoring emission at energy $E_m = 2.5$ eV: energy position of the peak maximum (E_m, eV), FWHM (ΔE, eV), amplitude (A, arb.units).

Parameters	Gaussian shape bands				
	G1	G2	G3	G4	G5
E_m	3.51	3.74	4.05	4.51	5.08
ΔE	0.27	0.32	0.26	0.44	0.47
A	58.2	85.1	52.2	17.1	2.5

Note. The peak amplitudes were normalized to 100 conventional units at the observed maximum (Fig. 3, curve 5).

List of Figure Captions

Figure 1. Absorption spectra of lanthanum beryllate single crystals. Experimental data recorded at $T = 293$ K for: (1) pristine undoped BLO; (2) BLO:Ce^{3+}; (3) BLO:Ce^{4+}; (4) BLO:Eu^{2+}. Dash line (5) shows the Urbach's tail of the host absorption in accordance with [20].

Figure 2. Absorption spectrum of BLO:Eu^{3+} (0.5 at %) single crystals recorded at $T = 80$ K.

Figure 3. Luminescence spectra of BLO:Ce^{3+} single crystals at $T = 80$ (1, 2, 5) and 290 K (3, 4, 6): PL emission spectra recorded upon excitation at $E_{ex} = 3.50$ (1, 3), 3.97 (2) and 4.43 eV (4); PL excitation spectra recorded monitoring emission at $E_m = 2.5$ eV (5, 6). The intensities of (1, 5, 6) spectra are normalized to unity. The 1–4 spectra are comparable in intensity. The dashed lines correspond to elementary Gaussian bands, solid smooth lines are the best fit.

Figure 4. Temperature dependence of PL intensity recorded for BLO single crystals doped with Ce^{3+} (1, 2) and Eu^{3+} (3) ions monitoring emission at 2.53 (1, 2), and 1.9–2.0 eV (3) upon excitation at 3.6 (1), 5.4 (2), and 3.1 eV (3).

Figure 5. PL emission spectra of BLO:Eu^{3+} single crystals recorded at $T = 80$ K with spectral resolution of 0.8 nm upon excitation at $E_{ex} = 3.90$ eV. Possible assignments for radiative transitions (1–5) were shown.

Figure 6. PL excitation spectra of BLO:Eu^{3+} single crystals recorded at $T = 80$ and 290 K monitoring emission in the energy range of 1.9–2.0 eV. Possible assignments for 4f–4f transitions (1–3) were shown. Vertical arrow indicates the energy threshold (E_{CT2}) for charge-transfer transitions O–Eu.

Figure 7. Diagram of the relaxation of low-energy electronic excitations in BLO single crystals doped with trivalent cerium or europium ions. The numbers indicate radiative transitions: (1) $^5D_0 \rightarrow {}^7F_{0-4}$ in Eu^{3+} ion; (3) $5d^1 \rightarrow {}^2F_{5/2}$, and (4) $5d^1 \rightarrow {}^2F_{7/2}$ in Ce^{3+} ion. Optical transitions are shown as: (2) $4f^1 \rightarrow 4f$ in Eu^{3+} and (5) $4f^1 \rightarrow 5d$ in Ce^{3+}. Charge-transfer transitions are shown as E_{CT1} and E_{CT2}.

Figure 8. The calculated energy level diagram of the lanthanides in BLO depending on the number of electrons in the ground state of the $4f^n$-configuration of the trivalent lanthanide ion. Curves 1 and 2 correspond to the lowest states of the $4f^n$ and $4f^{n-1}5d$-configurations of the trivalent lanthanides. Curves 3 and 4 correspond to the lowest levels of the $4f^{n+1}$ and $4f^n5d$-configurations of the divalent lanthanides. The arrows show the experimental data used to construct the diagram.

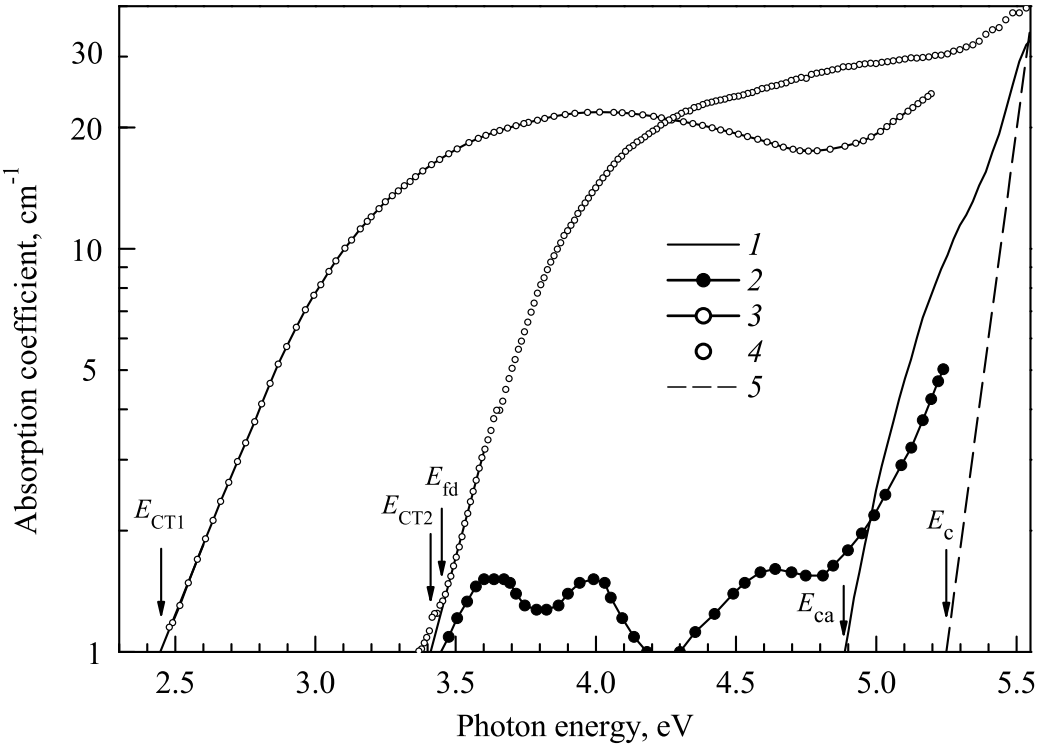

Figure 1: Absorption spectra of lanthanum beryllate single crystals. Experimental data recorded at $T = 290$ K for: (1) pristine undoped BLO; (2) BLO:Ce^{3+}; (3) BLO:Ce^{4+}; (4) BLO:Eu^{2+}. Dash line (5) shows the Urbach's tail of the host absorption in accordance with [20].

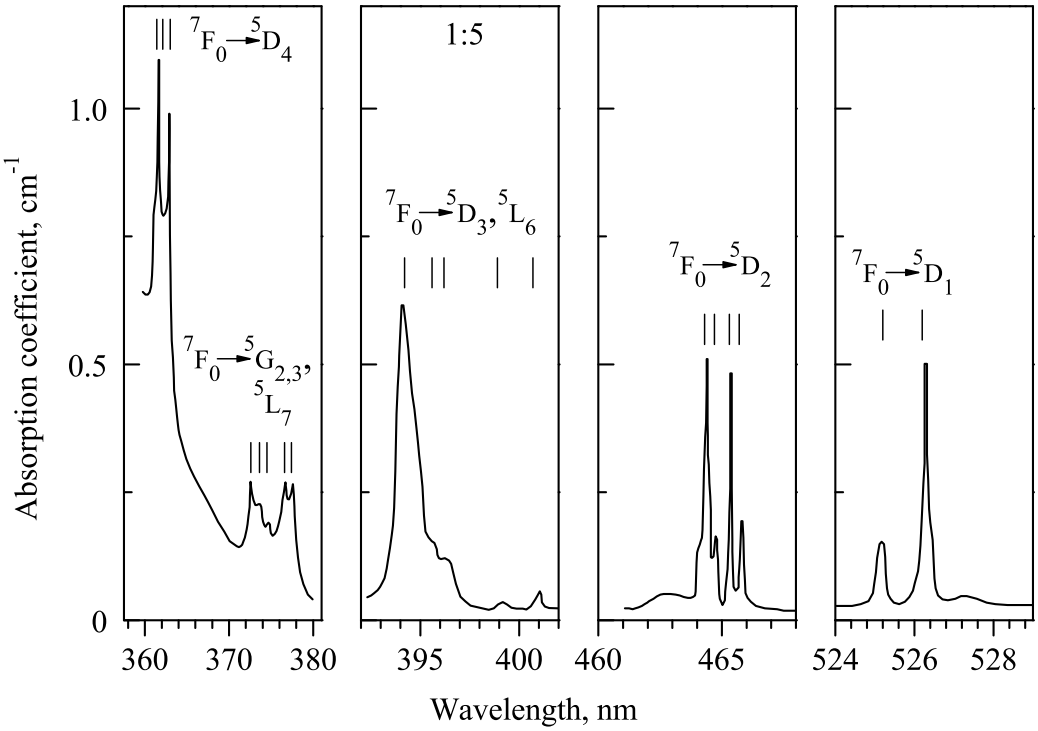

Figure 2: Absorption spectrum of BLO:Eu^{3+} (0.5 at %) single crystals recorded at $T = 80$ K.

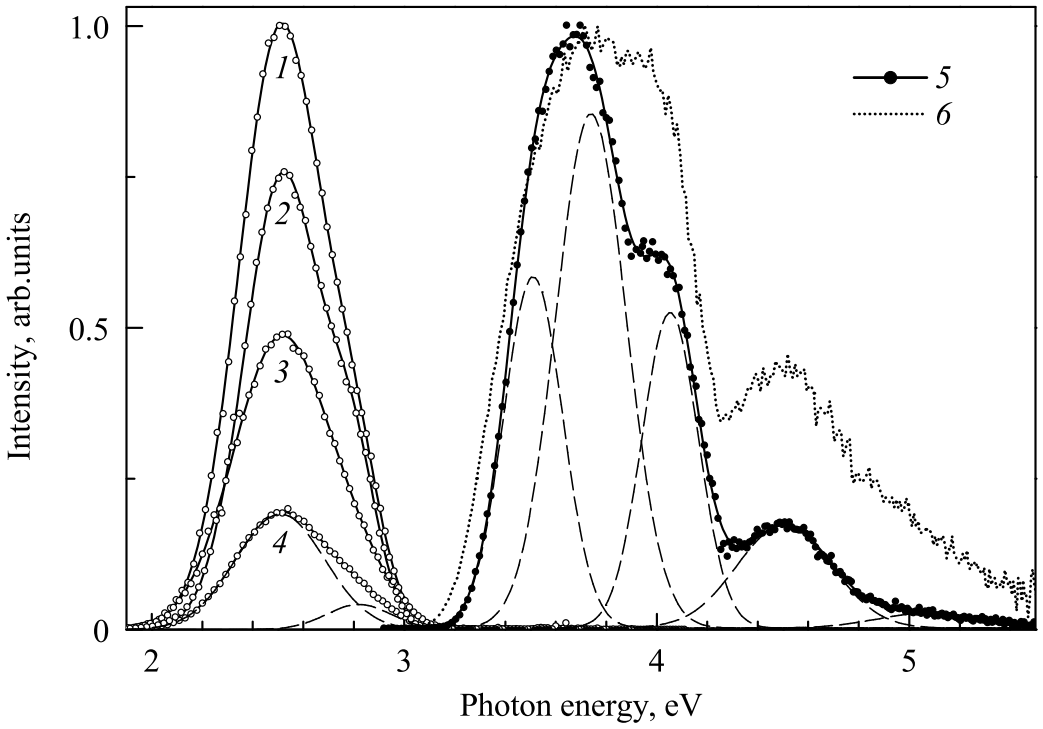

Figure 3: Photoluminescence spectra of BLO:Ce^{3+} single crystals at T= 80 (1, 2, 5) and 290 K (3, 4, 6): PL emission spectra recorded upon excitation at E_{ex}= 3.50 (1, 3), 3.97 (2) and 4.43 eV (4); PL excitation spectra recorded monitoring emission at E_m= 2.5 eV (5, 6). The intensities of (1, 5, 6) spectra are normalized to unity. The 1–4 spectra are comparable in intensity. The dashed lines correspond to elementary Gaussian bands, solid smooth lines are the best fit.

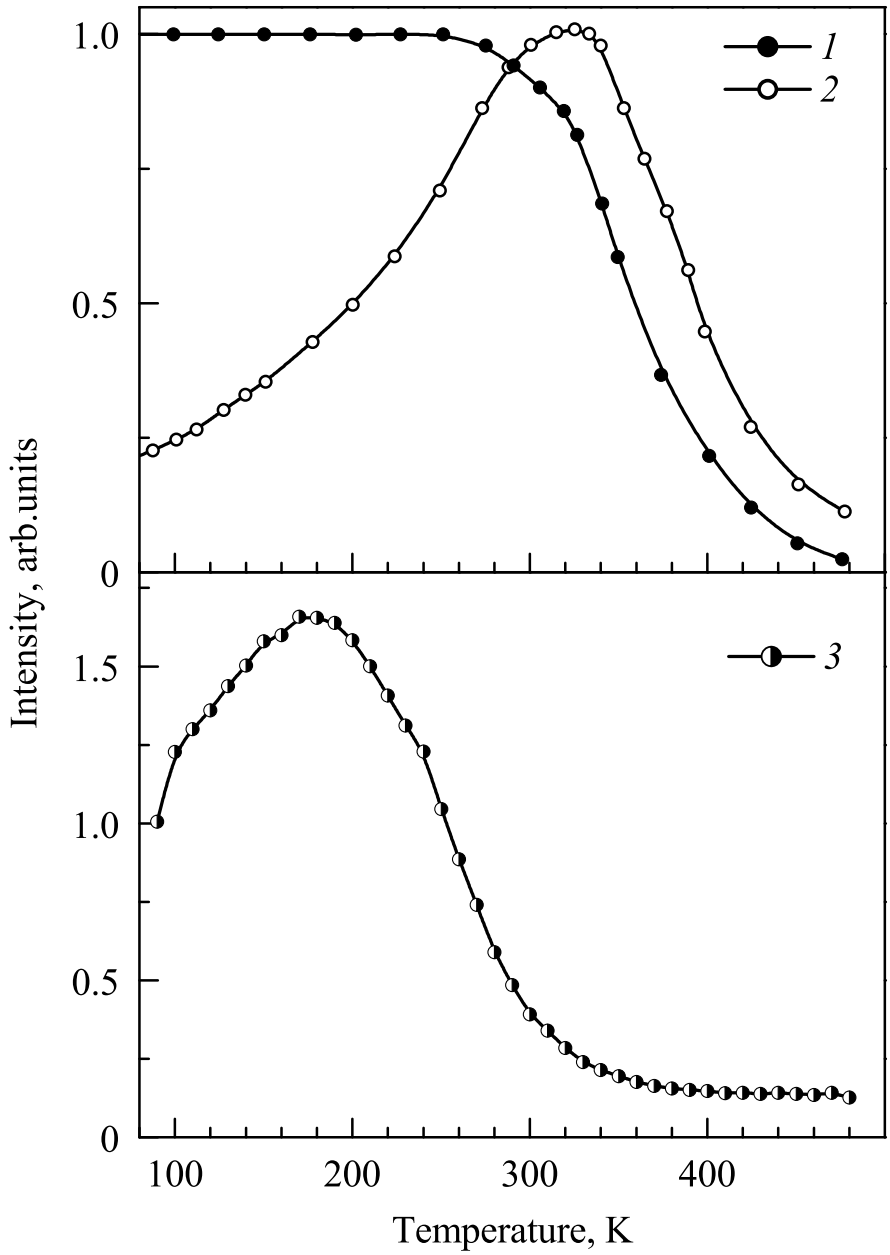

Figure 4: Temperature dependence of PL intensity recorded for BLO single crystals doped with Ce^{3+} (1, 2) and Eu^{3+} (3) ions monitoring emission at 2.53 (1, 2), and 1.9–2.0 eV (3) upon excitation at 3.6 (1), 5.4 (2), and 3.1 eV (3).

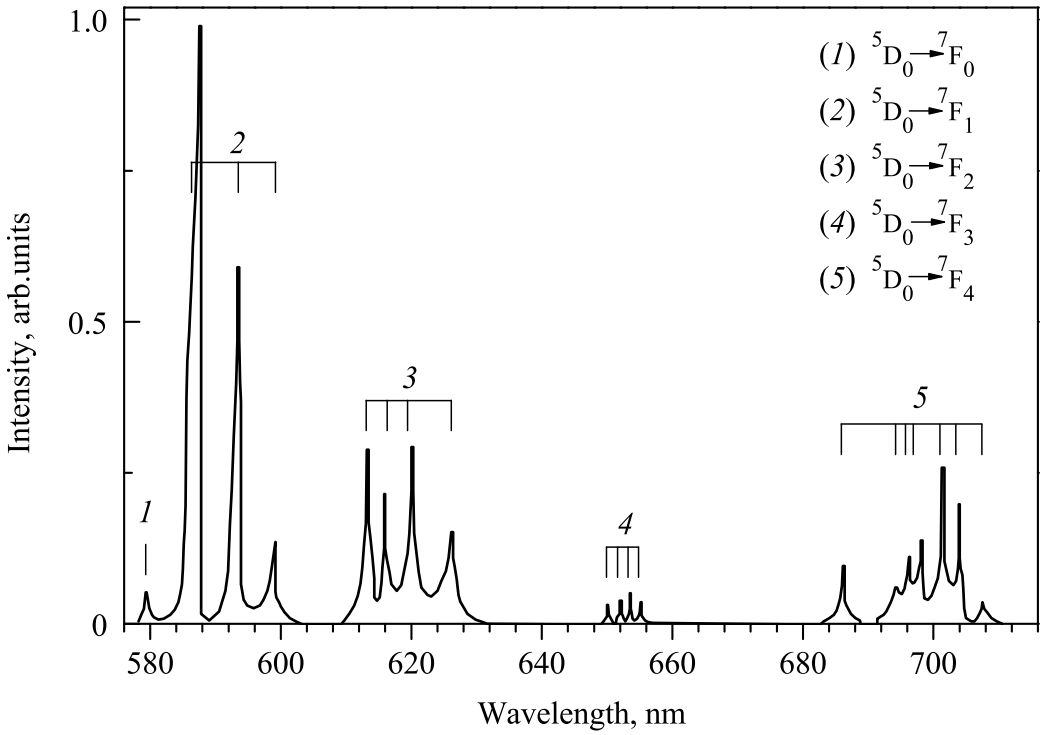

Figure 5: PL emission spectra of BLO:Eu^{3+} single crystals recorded at $T = 80$ K with spectral resolution of 0.8 nm upon excitation at $E_{ex} = 3.90$ eV. Possible assignments for radiative transitions (1–5) were shown.

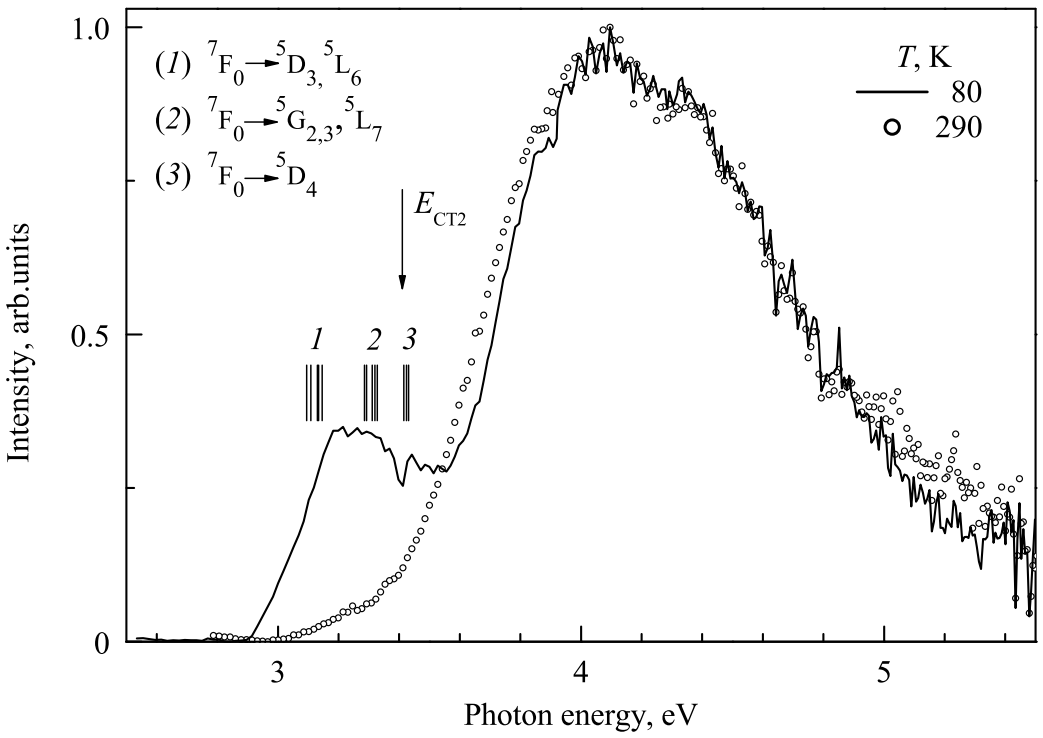

Figure 6: PL excitation spectra of BLO:Eu^{3+} single crystals recorded at $T = 80$ and 290 K monitoring emission in the energy range of 1.9–2.0 eV. Possible assignments for 4f–4f transitions (1–3) were shown. Vertical arrow indicates the energy threshold (E_{CT2}) for charge-transfer transitions O–Eu.

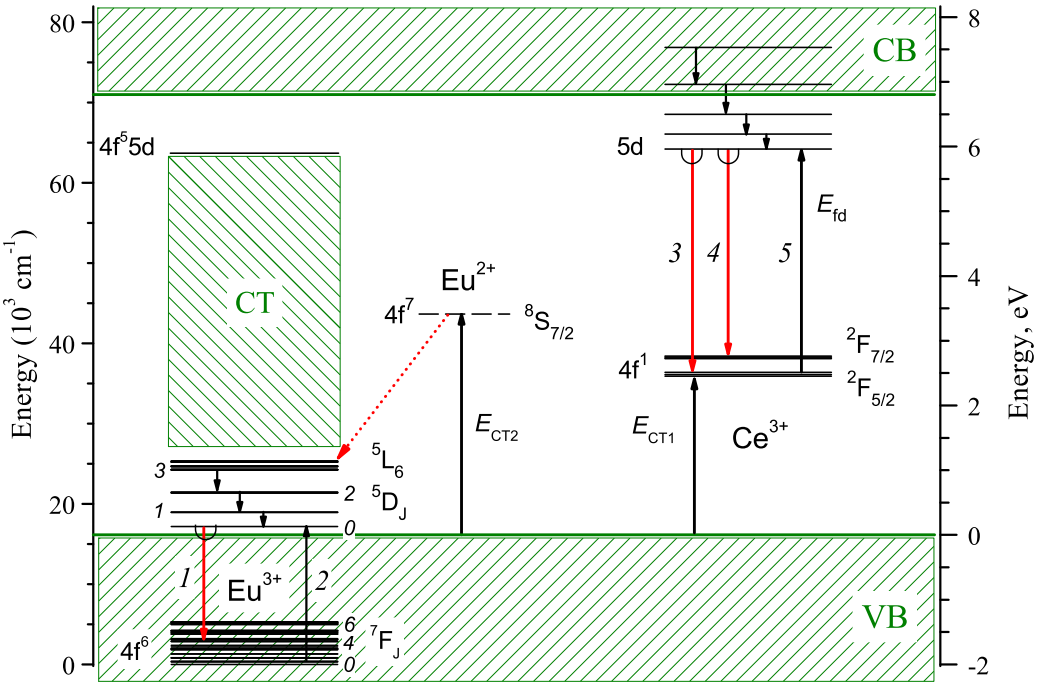

Figure 7: Diagram of the relaxation of low-energy electronic excitations in BLO single crystals doped with trivalent cerium or europium ions. The numbers indicate radiative transitions: (1) $^5D_0 \rightarrow {}^7F_{0-4}$ in Eu^{3+} ion; (3) $5d^1 \rightarrow {}^2F_{5/2}$, and (4) $5d^1 \rightarrow {}^2F_{7/2}$ in Ce^{3+} ion. Optical transitions are shown as: (2) $4f^1 \rightarrow 4f$ in Eu^{3+} and (5) $4f^1 \rightarrow 5d$ in Ce^{3+}. Charge-transfer transitions are shown as E_{CT1} and E_{CT2}.

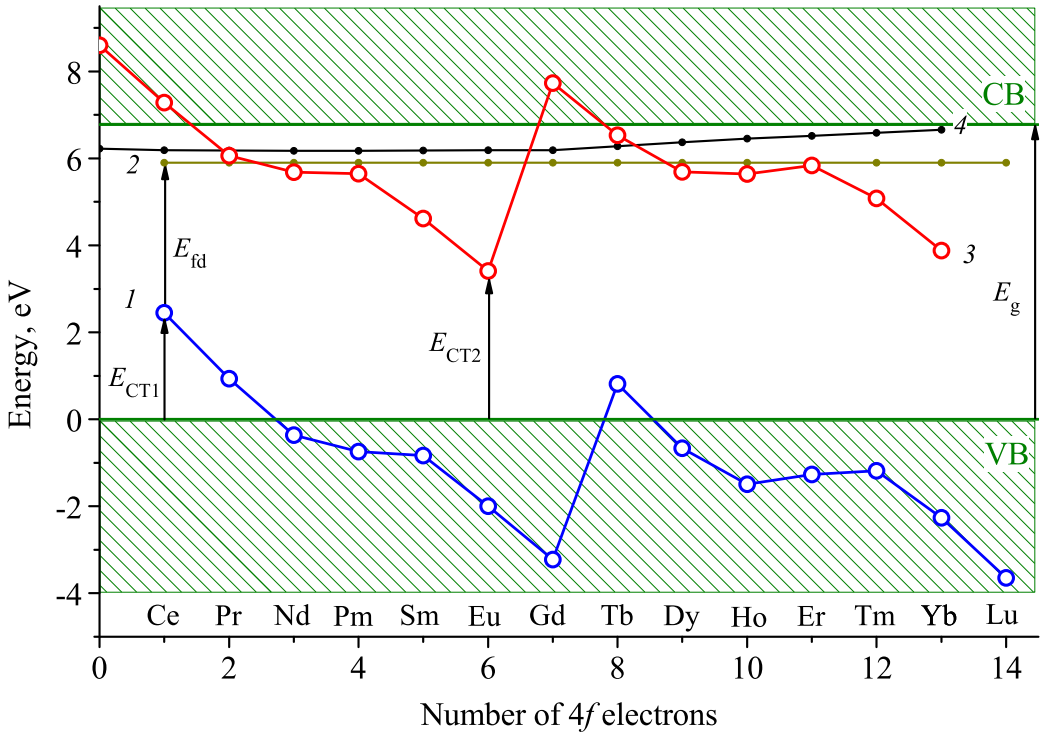

Figure 8: The calculated energy level diagram of the lanthanides in BLO depending on the number of electrons in the ground state of the $4f^n$-configuration of the trivalent lanthanide ion. Curves 1 and 2 correspond to the lowest states of the $4f^n$ and $4f^{n-1}5d$-configurations of the trivalent lanthanides. Curves 3 and 4 correspond to the lowest levels of the $4f^{n+1}$ and $4f^n5d$-configurations of the divalent lanthanides. The arrows show the experimental data used to construct the diagram.